J|A|C|S COMMUNICATIONS

Published on Web 04/24/2009

N Doping of Oxide Nanosheets

Yasumichi Matsumoto,* Michio Koinuma,* Yoshifumi Iwanaga, Tetsuya Sato, and Shintaro Ida

Graduate School of Science and Technology, Kumamoto University, 2-39-1 Kurokami, Kumamoto 860-8555, Japan

Received October 15, 2008; E-mail: yasumi@gpo.kumamoto-u.ac.jp; koinuma@chem.kumamoto-u.ac.jp

Semiconducting oxide nanosheets have many promising applications including photoluminescence, photocatalysis, and electrochemistry. The bandgaps of oxide nanosheets consisting of Ti−O, Nb−O, and Ta−O range from approximately 3.7 to 4.6 eV, where the valence and conduction bands consist of the p-orbital of O^{2-} and the d-orbital of the transition metal cations, respectively. Their bandgaps are large compared with those of the corresponding bulk crystals, because of quantum size effect. However, this large bandgap restricts the application of semiconducting oxide nanosheets. For example, only UV light with energy larger than the bandgap can be used as an excitation source in photocatalysis and photoluminescence. The bandgap energy of some semiconducting metal oxides can be decreased by modifications such as N doping,[1−14] where the p-orbital of the N dopant exists as a filled band near or hybridized with the p-valence band of O^{2-} in its original bandgap.[6,8,14] The N doping of oxide materials, however, is usually accomplished by a relatively complex process and/or harsh conditions using NH_3. In this work, we succeeded in the N doping of oxide nanosheets under mild conditions using UV light at room temperature.

The layered starting materials, $K_4Nb_6O_{17}$ (Nb−O), $KCa_2Nb_3O_{10}$ (Ca−Nb−O), $K_2Ti_4O_9$ (Ti−O), and $KTiNbO_5$ (Ti−Nb−O), for the preparation of the corresponding oxide nanosheets, were prepared by previously reported methods.[15−18] Crystal structures were confirmed using X-ray diffractometry (Cu Kα radiation, Rigaku RINT-2500VHF). All the layered samples were protonated by soaking and stirring in 2 M aqueous HCl solution for 3 days. The protonated samples were exfoliated in a solution of 0.05 M tetrabutylammonium hydroxide (TBA) to produce the nanosheets. After exfoliation, the suspension was centrifuged to separate the sediment and the nanosheet solution. Pt loading of the nanosheets was carried out via the addition of $PtCl_4$ (0.1%) and methanol (20%) to the nanosheet solution under the illumination of a 500 W Xe lamp for 1 h. The H-restacking of the nanosheets was carried out by the addition of dilute HNO_3 or HCl solution to the nanosheet solutions. The H-restacked samples 2 (without Pt loading) and 3 (with Pt loading) were used as the starting materials for photo-N doping (Supporting Information S1). The photo-N doping was performed for samples 2 and 3 in purified water excluding O_2 (in N_2 or Ar) under the illumination of a 500 W Hg lamp. UV light with energy greater than the bandgap was important for this process as no N doping occurred under visible light illumination (>390 nm). Characterization of the samples after N doping was performed using UV−vis absorption spectroscopy (diffuse reflection method, JASCO V-550), X-ray photoelectron spectroscopy (XPS, VG Scientific Sigma probe) and Fourier-transform infrared spectroscopy (FTIR, Perkin-Elmer). Atomic force microscopy (AFM, Nanoscope V Digital Instruments) was used to observe the lateral size of the nanosheets. (The lateral sizes of all the nanosheets prepared in this study were approximately 0.1−0.5 μm.) The photocatalytic activity of the nanosheets was measured in 200 cm^3 of 4 M aqueous methanol solution containing 0.1 g of the nanosheets under illumination. Methanol acted as a scavenger of the photoproduced holes, and the amount of H_2 produced during the illumination was measured by gas chromatography.

After the photo-N doping of the H-restacked Nb−O nanosheets in samples 2 and 3, the color changed from white to brown-yellow. Figure 1 shows the absorption spectra of the H-restacked sample 3

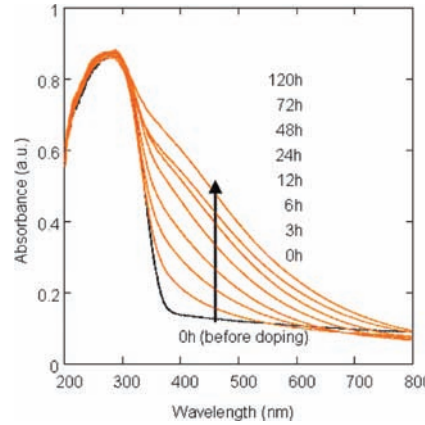

Figure 1. UV−vis absorption spectra of the restacked N doped Nb−O nanosheet sample loaded with Pt (sample 3 in Supporting Information S1). Visible absorbance increases with increasing illumination time.

of the Nb−O nanosheet after photo-N doping. Relatively strong visible absorption (approximately 400−600 nm) as well as UV absorption due to the Nb−O nanosheet bandgap (around <370 nm) appeared. The visible absorbance increased with increasing illumination time. Figure 2 shows the N1s XPS spectra of the Nb−O

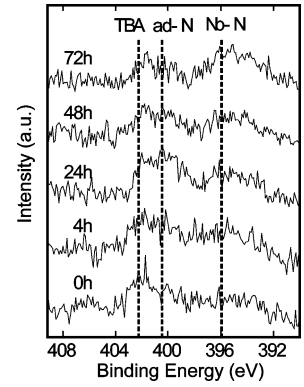

Figure 2. N1s XPS spectra of the restacked Nb−O sample loaded with Pt (sample 3 in Supporting Information S1) before (0 h) and after photo-N doping for 4, 24, 48, 72 h.

samples before and after photo-N doping. The characteristic binding energy of the N dopant (about 396 eV, existing as N^{3-}, N^-, N, or Nb−N)[8,9,13,19,20] was observed for the sample after the photo-N doping, while the binding energy of TBA (about 402 eV due to

10.1021/ja807388t CCC: $40.75

the N−C bond) was observed for the sample before the doping treatment. A binding energy of about 401 eV which is due to either O−N or adsorbed N,[9,19,21] appeared following N doping. These results clearly indicate that the N doping of the Nb−O nanosheet occurs. The content of the N dopant (as Nb−N) was about 3 atm % of all O atoms in the nanosheet after photo-N doping for 24 h, according to the XPS semiquantitative analysis using each measured peak area.

The photo-N doping also occurred for other Nb−O nanosheet systems such as Ca−Nb−O and Ti−Nb−O (Supporting Information S2), but did not occur for Ti−O nanosheets containing no Nb (Supporting Information S3). The removal of O_2 from the purified water (saturated with N_2 or Ar) during the photo-N doping process was also necessary for N doping to occur. This indicates that the photoreduction of O_2 suppresses the N doping. Moreover, the presence of TBA was necessary for this process. No N doping occurred when other amines such as ethylamine, dimethylamine, and trimethylamine were substituted for TBA as the exfoliation reagent. TBA in the H-restacked sample was immediately destroyed after photo-N doping based on an analysis of the FTIR spectrum. The peaks corresponding to C−H bonding in TBA disappeared after photo-N doping (Supporting Information S4). Pt loading promoted N doping, as determined from a comparison of the absorption spectra of samples 3 (Figure 1) and 2 (Supporting Information S5). No N doping of the nanosheets occurred when illuminating the nanosheet solutions (sample 1 in Supporting Information S1). This indicates that the restacked form (samples 2 and 3) with aggregation of the nanosheets is very important for this N-doping process.

Photo-N doping will occur on the surface of the nanosheets attached to the edge of other Nb−O system nanosheets in the restacked forms, where the edge serves as the photoreduction site. At the first step, TBA will be decomposed by hole on the surface of the nanosheets to form some active intermediate. At the second step, it will be reduced by electron at the edge of the nanosheet[22] to bring about the N doping on the surface of another nanosheet (Supporting Information S6). O_2 will be preferentially reduced by electron at the edge during the second step, leading to the suppression of the N doping. At the edge of the nanosheets, Pt acts as a catalyst during the above photoreduction reaction.[23] The conduction band of the Nb−O system is in a higher energy position than those of the Ti−O system, and will be more suitable for the above process, because the electron produced in the conduction band of the Nb−O system is more active for the photoreduction reaction. Consequently, Nb−O nanosheets act as their own photocatalyst in the H-restacked form during this photo-N doping process. N doping was observed for a mixed H-restacked sample consisting of Nb−O and Ti−O nanosheets (Ti−O 90%, Nb−O 10%), although no doping occurred for the sample with only Ti−O nanosheets (Supporting Information S3). The visible absorption intensity around 450 nm for the mixed sample illuminated for 24 h was much higher than that of calculated visible absorption, where the ratio of the visible absorption to the maximum bandgap absorption was calculated to be 10% using spectrum of the N-doped sample for 24 h (Figure 1). This means that some Ti−O nanosheets attached to the edges of the Nb−O nanosheets are doped with N in the mixed samples.

The photocatalytic activity of the N-doped Nb−O nanosheet for water photolysis was evaluated by measuring the H_2 generated under visible light (>420 nm). The reaction proceeded for the N-doped nanosheet, while no H_2 evolution occurred for the nondoped Nb−O nanosheet under the same conditions (Supporting Information S7). Thus, the electron produced by excitation from the N-band to the d-conduction band in the N-doped nanosheet brings about the reduction of water to H_2. The photocatalytic activity slightly decreased after 12 h photolysis test under visible light (Supporting Information S7). The content of the doped N also decreased with an increase of the photolysis time, and its degree was large for the UV illumination (Supporting Information S8).

In conclusion, we have succeeded in developing a simple method for the N doping of Nb−O nanosheets under mild conditions, where UV light with energy greater than the bandgap was used as the illumination source in the presence of TBA at room temperature. The Nb−O nanosheets act as a photocatalyst in this N-doping process. Long illumination times (>80 h) for the doping in Ar brought about a decrease in the visible absorption, suggesting that N_2 may possibly act as a doping source. Therefore, a study investigating the details of the mechanism of this photo-N doping process is now in progress.

Acknowledgment. This work was supported by a Grant-in-Aid for Scientific Research (A) (No. 19205025) from Japan Society for the Promotion of Science.

Supporting Information Available: S1: preparation scheme, S2, S3, S4, S8: UV−vis absorption data, S4: FT-IR data, S6; mechanism model, and S7: amounts of photoproduced H_2 under visible light illumination. This material is available free of charge via the Internet at http://pubs.acs.org.

References

(1) Sato, S. *Chem. Phys. Lett.* **1986**, *123*, 126.
(2) Asahi, R.; Morikawa, T.; Ohwaki, T.; Aoki, K.; Taga, Y. *Science* **2001**, *293*, 269.
(3) Chen, X.; Burda, C. *J. Phys. Chem. B* **2004**, *108*, 15446.
(4) Sathish, M.; Viswanathan, B.; Viswanath, R. P.; Gopinath, C. S. *Chem. Mater.* **2005**, *17*, 6349.
(5) Torres, G. R.; Lindgren, T.; Lu, J.; Granqvist, C.-G.; Linquist, S.-E. *J. Phys. Chem. B* **2004**, *108*, 5995.
(6) Nakamura, R.; Tanaka, T.; Nakato, Y. *J. Phys. Chem. B* **2004**, *108*, 10617.
(7) Mrowetz, M.; Balcerski, W.; Colussi, A. J.; Hoffmann, M. R. *J. Phys. Chem. B* **2004**, *108*, 17269.
(8) Batzill, M.; Molares, E. H.; Diebold, U. *Phys. Rev. Lett.* **2006**, *96*, 026103.
(9) Chen, H.; Nambu, A.; Wen, W.; Graciani, J.; Zhong, Z.; Hanson, J. C.; Fujita, E.; Rodriguez, J. A. *J. Phys. Chem. C* **2007**, *111*, 1366.
(10) Jansen, M.; Letschert, H. P. *Nature (London)* **2000**, *404*, 980.
(11) Cong, Y.; Zhang, J.; Chen, F.; Anpo, M. *J. Phys. Chem. C* **2007**, *111*, 6976.
(12) Kim, Y.; Woodward, P. M.; Baba-Kishi, K. Z.; Tai, C. W. *Chem. Mater.* **2004**, *16*, 1267.
(13) Murase, T.; Irie, H.; Hashimoto, K. *J. Phys. Chem. B* **2004**, *108*, 15803.
(14) Hitoki, G.; Takata, T.; Kondo, J. N.; Hara, M.; Kobayashi, H.; Domen, K. *Chem. Commun.* **2002**, 1698.
(15) Wadsley, A. D. *Acta Crystallogr.* **1964**, *17*, 623.
(16) Izawa, H.; Kikkawa, S.; Koizumi, M. *J. Phys. Chem.* **1982**, *86*, 5023.
(17) Kudo, A.; Tanaka, A.; Domen, K.; Murayama, K.; Aika, K.; Onishi, T. *J. Catal.* **1988**, *111*, 67.
(18) Constantino, V. R. L.; Bizeto, M. A.; Brito, H. F. *J. Alloys Compd.* **1998**, *278*, 142.
(19) Saha, N. C.; Tompkins, H. G. *J. Appl. Phys.* **1922**, *72*, 3072.
(20) Diwald, O.; Tompson, T. L.; Goralski, E. G.; Walck, S. D.; Yates, J. K., Jr. *J. Phys. Chem. B* **2004**, *108*, 15446.
(21) Ma, T.; Akiyama, M.; Abe, E.; Imai, I. *Nano Lett.* **2005**, *5*, 3543.
(22) (a) Matsumoto, Y.; Ida, S.; Inoue, T. *J. Phys. Chem. C* **2008**, *112*, 11614. (b) Unpublished data, where it is confirmed that the photoreduction site of $Ca_2Nb_3O_{10}$ nanosheet is the edge, because the photodeposition of Cu occurs only at the edge.
(23) Compton, C. O.; Carroll, C. E.; Kim, J. Y.; Larsen, D. S.; Osterloh, F. E. *J. Phys. Chem. C* **2007**, *111*, 14589.

JA807388T